International Journal of Technology (2016) 8: 1307-1315
ISSN 2086-9614

PERFORMANCE OF VANADIUM-DOPED $LiFePO_4$/C USED AS A CATHODE FOR A LITHIUM ION BATTERY

Nofrijon Sofyan[1,2*], Dimas Yunianto Putro[1], Anne Zulfia[1,2]

[1]*Department of Metallurgy and Materials Engineering, Faculty of Engineering, Universitas Indonesia, Kampus UI Depok, Depok 16424, Indonesia*
[2]*Tropical Renewable Energy Center, Faculty of Engineering, Universitas Indonesia, Kampus UI Depok, Depok 16424, Indonesia*

(Received: November 2016 / Revised: December 2016 / Accepted: December 2016)

ABSTRACT

Vanadium-doped $LiFePO_4$/C used as a cathode for a lithium ion battery has been successfully synthesized. In this work, $LiFePO_4$ was synthesized from LiOH, $NH_4H_2PO_4$, and $FeSO_4$.7H2O at a stoichiometric amount. Vanadium was added in the form of H_4NO_3V at concentration variations and 3 wt.% carbon black. The characterization includes thermal analysis, X-ray diffraction, electron microscopy, and electrical impedance spectroscopy. The thermal analysis results showed that the $LiFePO_4$ formation temperature is 653.8–700.0°C. The X-ray diffraction results showed an olivine structure with an orthorhombic space group, whereas the electron microscopy results showed that $LiFePO_4$/C has a round shape with an agglomerated microstructure. Electrical impedance test results showed values of 158 Ω and 59 Ω for the as-synthesized $LiFePO_4$/C and the 5 wt.% vanadium-doped $LiFePO_4$/C, respectively. Cyclic performance test results at 1 C showed capacities of 24.0 mAh/g and 31.2 mAh/g for the as-synthesized $LiFePO_4$/C and the 5 wt.% vanadium-doped $LiFePO_4$/C, respectively. Charge and discharge test results showed charge and discharge capacities of 27.6 mAh/g and 40.2 mAh/g for the as-synthesized $LiFePO_4$/C and the 5 wt.% vanadium-doped $LiFePO_4$, respectively. This result is promising in terms of increasing the performance of a lithium ion battery.

Keywords: Doping; Hydrothermal method; $LiFePO_4$; $LiFeVPO_4$; Lithium ion battery

1. INTRODUCTION

At the beginning of its invention, the lithium battery provided a significant performance improvement in terms of weight, capacity, and power (Han et al., 2014). However, its high cost, safety hazards, and chemical instability prohibited its extensive applications (Belharouak et al., 2011). Therefore, many researchers have investigated ways to overcome these problems (Padhi et al., 1997; Li et al., 2011; Nagakane et al., 2012). The discovery of the lithium ion battery was based on lithium ions being able to move between the layers of certain atoms in the crystal, a process known as intercalation (Belharouak et al., 2011). Lithium ion battery cells utilize the Volta principle to move lithium ions from the cathode to the anode during charging and then backward from the anode to the cathode during usage (Li et al., 2011).

Currently, lithium ion phosphate ($LiFePO_4$) is among the various cathode materials used in lithium ion batteries, and $LiFePO_4$ is getting more attention due to its environmental friendliness, low cost, and long cycle, particularly in nano-sizes for better safety and higher

---

*Corresponding author's email: nofrijon.sofyan@ui.ac.id, Tel. + 62-21-7863510, Fax. +62-21-7872350
Permalink/DOI: https://doi.org/10.14716/ijtech.v7i8.6893

theoretical capacity (Zhong & Zhou, 2010; Wang et al., 2014). This material can be synthesized in several ways, such as sol-gel (Hsu et al., 2004; Yang & Xu, 2004), hydrothermal (Deng et al., 2012; Wang et al., 2013; Yu et al., 2014), and solvothermal (Cho et al., 2013; Zhou et al., 2013). Among these methods, hydrothermal is one of the choices that can be used to obtain $LiFePO_4$ with relatively high purity. Lithium iron phosphate has a low electronic conductivity of about 10 S/c^{-9}, which causes low rate capabilities (Chung et al., 2002). Investigators have proposed numerous approaches to improve this electrical conductivity, such as using a nanoscale material, doping with other materials, and using carbon coating (Väyrynen & Salminen, 2012). Adding carbon through the hydrothermal pathway is expected to form a composite $LiFePO_4$/C with more conductivity. To further improve the electro-chemical performance of $LiFePO_4$ cathode material, the introduction of a second dopant has been proposed in the literature (Yang et al., 2015).

In this present work, vanadium-doped LiFePO4/C cathode materials have been synthesized via a hydrothermal method. The effects of vanadium doping on the structure, morphology, and electrochemical performance of $LiFePO_4$/C are studied and discussed in detail.

2. EXPERIMENTAL METHOD

2.1. Synthesis of $LiFePO_4$

In this work, $LiFePO_4$ was prepared from LiOH, $NH_4H_2PO_4$, and $FeSO_4.7H_2O$, all grade reagents from E-Merck. The three precursors were diluted with 30 ml distilled water in a separated glass beaker. After being mixed with distilled water, the three solutions of LiOH, $NH_4H_2PO_4$, and $FeSO_4.7H_2O$ were mixed into a glass beaker and stirred until homogenized under a magnetic stirrer for 30 minutes. The solution was transferred into a Teflon autoclave and heated in a furnace at 180ºC for 20 hours. After the heating process, the solution was transferred into a beaker and left to form precipitate. The precipitate was separated from the solution and washed with deionized water before being dried in an oven at 80ºC for 18 hours.

2.2. Synthesis $LiFePO_4$/V/C

In this step, the $LiFePO_4$ powders from the previous step were prepared with 3 wt.% carbon black and variations of 0, 3, 5, and 7 wt.% H_4NO_3V. First, the $LiFePO_4$ and H_4NO_3V powders were ball milled until homogenized, and then the carbon black was added and the ball-milling process continued until a homogenized mix was obtained. After the milling process, a small amount of specimen was tested with a thermal analyzer (PerkinElmer STA 6000) to examine the crystallization process. The results from the thermal analysis showed that the sintering process needs to be performed at 700ºC. Therefore, all the samples were then sintered at 700ºC for four hours under a nitrogen environment. The characteristics of the resulting cathode materials were examined by using X-ray diffraction (XRD, Philips PW3020) with Cu Kα radiation (λ = 1.5406 Å) and a field emission scanning electron microscope (FE-SEM, FEI Inspect F50).

2.3. Battery Preparation

The active material from the previous step was applied onto an aluminum cathode sheet (MTI) and hot-rolled and heated at 80°C. For the electrochemical test, 80 wt.% as-prepared $LiFePO_4$ material was mixed with poly-vinylidene fluoride (PVDF) in N-methyl pyrrolidone (NMP) solvent inside a vacuum mixer. The solution was applied on aluminum foil and then dried. After drying, the sample was hot-rolled and heated in a vacuum oven at 80°C. The battery was prepared in the form of a coin by using an Li metal anode for half-cell, and $LiPF_6$ was used as an electrolyte solution. The cell was then tested through charge/discharge by using MTI battery analyzer equipment (EIS, Hioki LCR 3532-50).

3. RESULTS AND DISCUSSION

The curves from thermal analysis can be seen from Figure 1. The TG curve consists of three stages. In the first stage, at temperature 60-200°C, there is a slight increase in mass due to the formation of Li_3PO_4 and $Fe_3(PO_4)_2$, followed by water evaporation resulting in a decrease of mass at temperature 200-335°C. This phenomenon is also characterized by a small streak at 60-335°C, culminating at 235°C in the DTA curve. Therefore, $LiFePO_4$ decomposition would not occur at this temperature range. In the second part, at 335°C, the weight increases up to 650°C and then decreases due to carbon oxidation. The exothermic reaction occurs at around 700°C, indicating the crystallization of $LiFePO_4$. After this, increasing the temperature results in an endothermic reaction, indicating an oxide decomposition of $LiFePO_4$ back to $Li_3Fe_2(PO4)_3$ and Fe_2O_3 (Li et al., 2011). The next stage is a constant plane with a slight weight reduction to continue the oxidation of $LiFePO_4$. This result agrees with other studies that found olivine $LiFePO_4$ will oxidize into $Li_3Fe_2(PO4)_3$ and Fe_2O_3 (Deng et al., 2012; Tan et al., 2014). This formation temperature of $LiFePO_4$ is slightly different from that obtained by Franger et al. (2003), who determined it to be at 550°C with the addition of carbon less than 5 wt.%, and Belharouak et. al. (2005), who determined it to be at 450°C. This difference is expected to be due to the type of starting materials and the synthesis routes.

To confirm the phases obtained from the sintering process, an XRD test was performed on all samples. The diffraction pattern is shown in Figure 2. All samples synthesized at various conditions, showing the same diffraction patterns with that of the references (Yang & Ke, 2008; Teng et al., 2007): olivine structure indexed to the orthorhombic Pnma space group (JCPDS 83-2092). No typical diffraction peaks of carbon nor vanadium are found. This indicates that carbon exists in an amorphous form and that vanadium occupies Fe sites in $LiFePO_4$ or have been dissolved into $LiFePO_4$ to form a solid solution. The peaks, however, show a slight shifting toward a low angle with the increase of vanadium content (Franger et al., 2003). This is expected since vanadium has a larger radius than iron; thus, a higher vanadium content will affect the lattice parameters. With the change of the lattice parameters, there will be a change in the volume of the unit cell, which is slightly larger than that of the pristine $LiFePO_4/C$; thus, it will provide more space for the intercalation and de-intercalation processes (Yang et al., 2015).

A field emission electron scanning microscope was used to characterize the samples' morphology, and the results are given in Figure 3. No significant difference is observed in the materials' morphology between the as-synthesized and the vanadium-doped samples. In Figure 3a, most of the particles in the as-synthesized $LiFePO_4/C$ are round but agglomerated, which is the characteristic of $LiFePO_4$ mixed with carbon black and formed through a hydrothermal process (Shu et al., 2012). Figure 3b is the morphology of 3 wt.% vanadium-doped $LiFePO_4/C$, and it has a round shape with a smaller particle size than that of the as-synthesized $LiFePO_4/C$ and the agglomerated one. In Figure 3c, the morphology of 5 wt.% vanadium-doped $LiFePO_4/C$ is shown. Figure 3d shows the morphology of 7 wt.% vanadium-doped $LiFePO_4/C$.

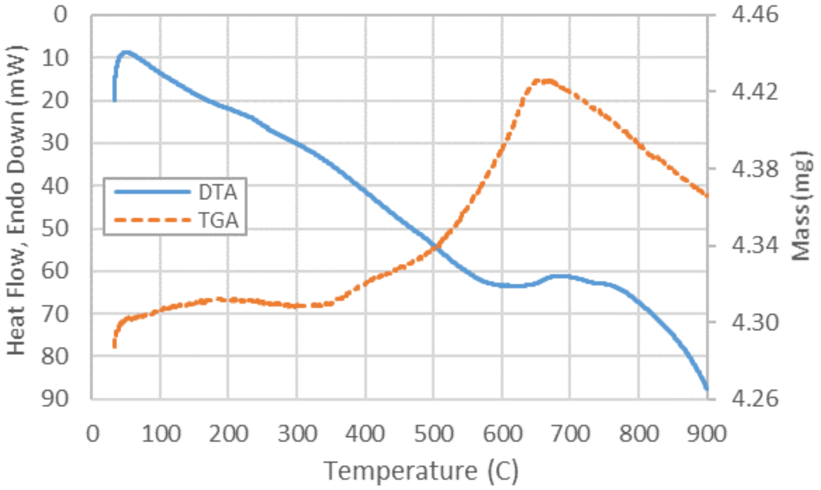

Figure 1 DTA and TGA graphs of the as-synthesized LiFePO$_4$/C

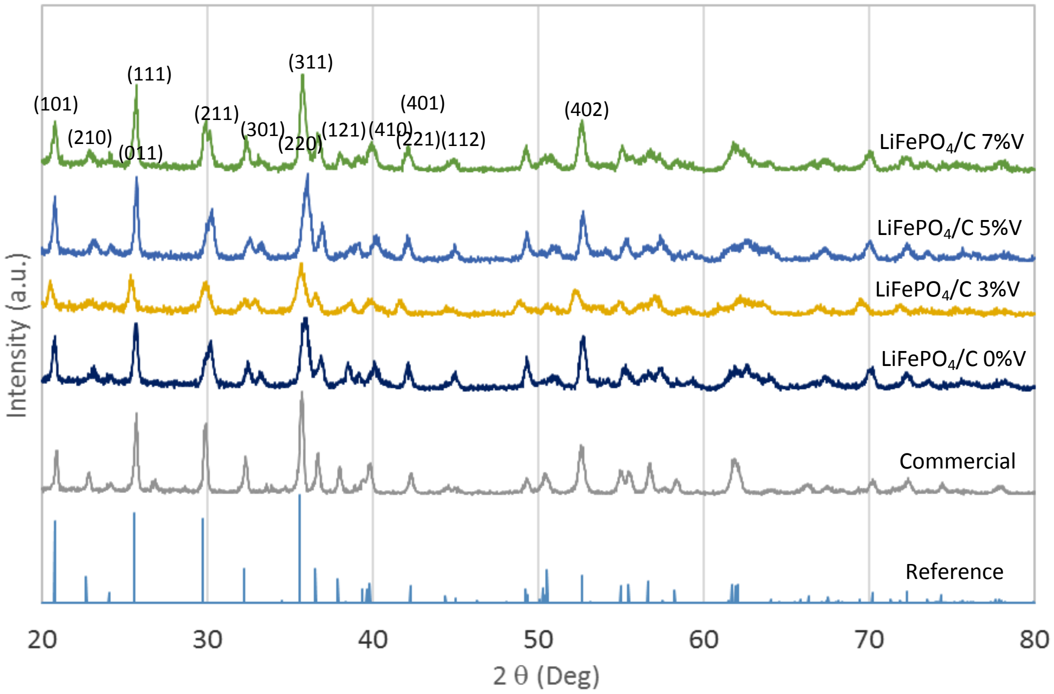

Figure 2 Diffraction patterns of reference, commercial, as-synthesized, 3 wt.%, 5 wt.%, and 7 wt.% vanadium-doped LiFePO$_4$/C

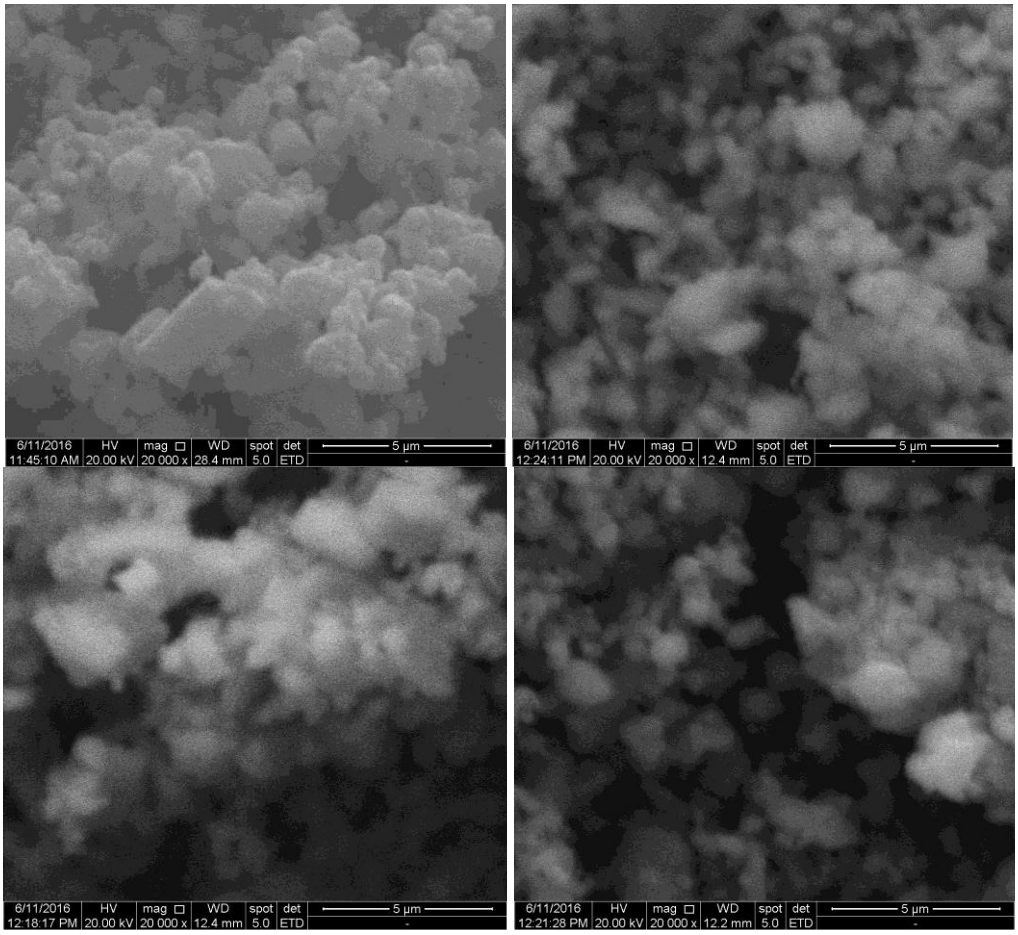

Figure 3 Secondary electron images of the samples: (a) as-synthesized; (b) 3 wt.% V-doped; (c) 5 wt.% V-doped; and (d) 7 wt.% V-doped $LiFePO_4/C$

It seems from the figures that the more the concentration of vanadium, the more the agglomeration found in the distribution of the particles in the microstructure. ImageJ analysis (Abramoff et al., 2004) on the microstructure of the as-synthesized $LiFePO_4/C$, 3 wt.%, 5 wt.%, and 7 wt.% vanadium-doped $LiFePO_4/C$ showed that the average particle size decreases with the increase of vanadium content. The average particle sizes of the as-synthesized $LiFePO_4$, 3 wt.%, 5 wt.%, and 7 wt.% vanadium-doped $LiFePO_4$ are around 200 nm, 120 nm, 100 nm, and below 100 nm, respectively. It seems that doping with vanadium reduces the interaction of $LiFePO_4/C$ particles to form large particles during the ball milling and further hinders growth during the sintering stage; however, the exact reason for this phenomenon has yet to be verified. Electrical impedance spectroscopy (EIS) testing of the active material showed the conductivity and Nyquist plot diagram depicting the material's capacitance. The test was performed on only two samples, i.e., the as-synthesized and the 5 wt.% vanadium-doped $LiFePO_4/C$. The results are given in Figure 4. The resistance of the sample on 5 wt.% vanadium-doped $LiFePO_4$ has a smaller value than that of the as-synthesized $LiFePO_4/C$. Imaginary impedance (Z') for the as-synthesized and the 5 wt.% vanadium-doped $LiFePO_4/C$ are 158 Ω and 59 Ω, respectively. From the impedance differences, the addition of vanadium on the $LiFePO_4$ cathode has a significant effect in increasing the active materials' conductivity.

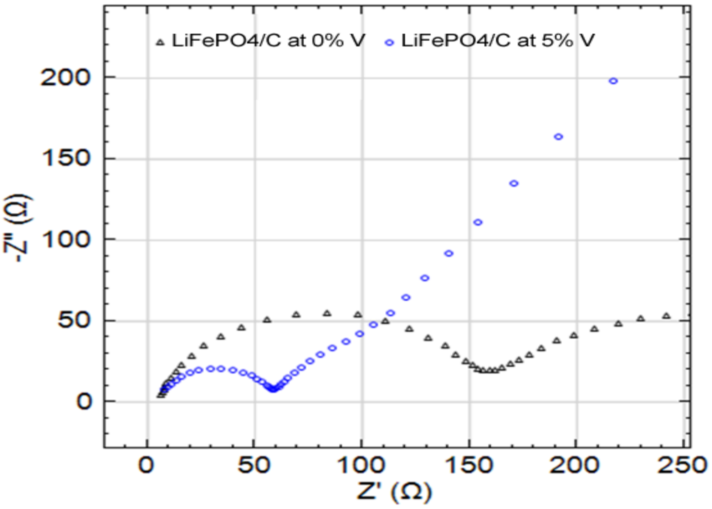

Figure 4 Nyquist plots of EIS test results for the as-synthesized (black triangle) and 5 wt.% vanadium-doped $LiFePO_4$/C (blue circle)

Figure 5 shows the results of a cyclic voltammetry test on the as-synthesized (a) and the 5 wt.% vanadium-doped $LiFePO_4$/C (b). As seen in Figure 5a for the as-synthesized $LiFePO_4$/C, the reduction-oxidation (redox) peak voltages are at 3.65 and 3.22 volts, respectively, whereas for the 5 wt.% vanadium-doped $LiFePO_4$/C, the reduction-oxidation (redox) peak voltages are at 3.62 and 3.28 volts, respectively.

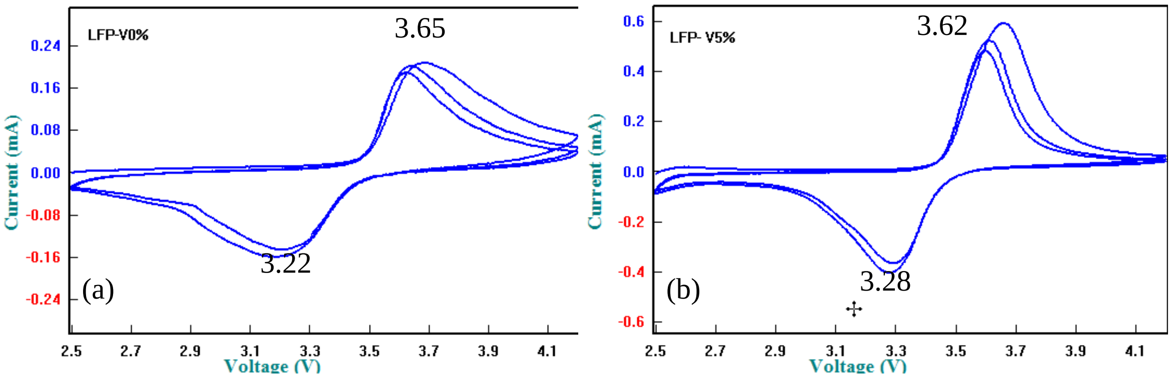

Figure 5 Cyclic voltammetry test results on samples of: (a) the as-synthesized; and (b) 5 wt.% vanadium-doped $LiFePO_4$/C

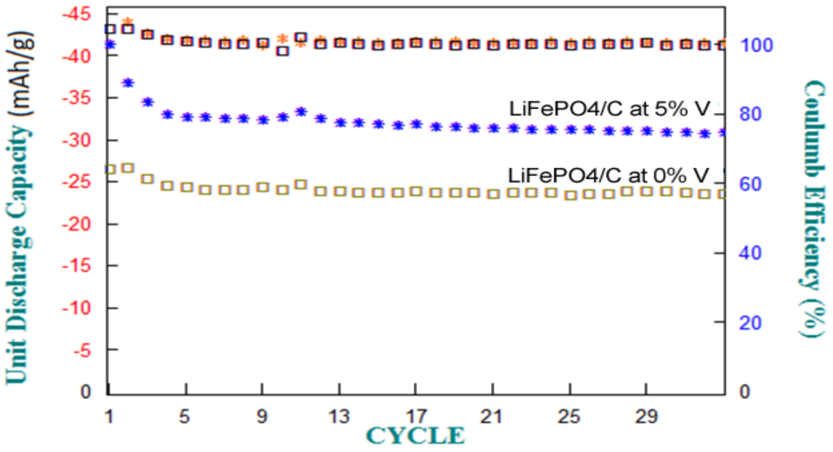

Figure 6 Cycle performance of the as-synthesized and the 5 wt.% vanadium-doped $LiFePO_4$/C at 1 C

A cycle performance test of up to 30 cycles for each of the samples is given in Figure 6. Cycle performance at 1 C for the as-synthesized and the 5 wt.% vanadium-doped $LiFePO_4$/C are about 24.0 mAh/g and 31.2 mAh/g, respectively.

Figure 7 shows the charge and discharge curves at various current densities for the as-synthesized and vanadium-doped $LiFePO_4$/C samples in the potential range of 2.5–4.0 V at room temperature. Vanadium greatly improves the discharge capacity of $LiFePO_4$/C. The initial discharge capacities of the as-synthesized $LiFePO_4$/C at 0.2 C (27.6 volts) increase with 5 wt.% vanadium-doped $LiFePO_4$/C (40.25 volts). The value decreases with the increase of current density, in which at 0.5, 2, 4, and 8 C the discharge capacities of the as-synthesized $LiFePO_4$/C are 19.41, 12.21, 7.20, and 3.23 volts, respectively; whereas the discharge capacities of 5 wt.% vanadium-doped $LiFePO_4$/C are 27.00, 18.05, 13.00, and 4.91, respectively.

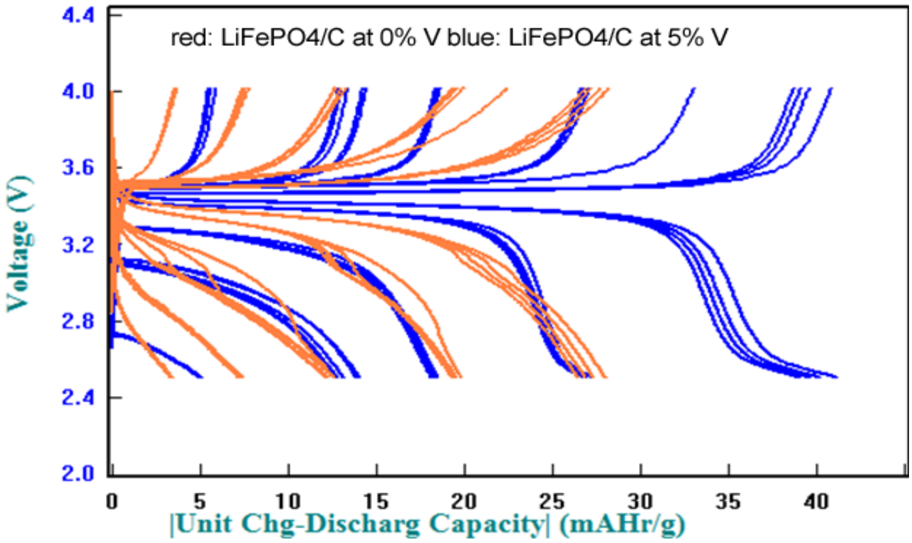

Figure 7 Charge/discharge test results in the potential range of 2.5–4.0 V at room temperature of the as-synthesized (red line) and the 5 wt.% vanadium-doped (blue line) $LiFePO_4$/C under current density of 0.2, 0.5, 2, 4, and 8 C

4. CONCLUSION

The hydrothermal process has been successfully carried out to synthesize $LiFePO_4$ with a light gray color, whereas the sintering process results in a dark gray color, as the characteristics of pure $LiFePO_4$ particles formed between 653.8~750.0°C. The EIS test results showed the impedance of the as-synthesized $LiFePO_4$/C and the 5 wt.% vanadium-doped $LiFePO_4$/C as 158 Ω and 59 Ω, respectively. The cyclic performance test results showed a capacity of 24.0 mAh/g and 31.2 mAh/g for the as-synthesized $LiFePO_4$/C and the 5 wt.% vanadium-doped $LiFePO_4$/C, respectively. The charge and discharge test results at 0.2 C showed that the discharge capacities of the as-synthesized and the 5 wt.% vanadium-doped $LiFePO_4$/C are 27.6 mAh/g and 40.2 mAh/g, respectively. These results are promising in terms of developing the cathode active material for a lithium ion battery.

5. ACKNOWLEDGEMENT

The authors would like to express their gratitude for the funding from the Directorate of Research and Community Services (DRPM), Universitas Indonesia, under Hibah Riset Kluster No. 1869/UN2.R12/HKP.05.00/2015.

6. REFERENCES

Abramoff, M.D., Magalhaes, P.J., Ram, S.J., 2004. Image Processing with ImageJ. *Biophotonics International*, Volume 11(7), pp. 36–42

Belharouak, I., Johnson, C., Amine, K., 2005. Synthesis and Electrochemical Analysis of Vapor-deposited Carbon-coated $LiFePO_4$. *Electrochemistry Communications*, Volume **7**(10), pp. 983–988

Belharouak, I., Koenig Jr., G.M., Amine, K. 2011. Electrochemistry and Safety of $Li_4Ti_5O_{12}$ and Graphite Anodes Paired with $LiMn_2O_4$ for Hybrid Electric Vehicle Li-ion Battery Applications. *Journal of Power Sources*, Volume 196(23), pp. 10344–10350

Cho, M., Kim, K., Lee, J., Kim, H., Kim, H., Kang, K., Roh, K.R., 2013. Defect-free Solvothermally Assisted Synthesis of Microspherical Mesoporous $LiFePO_4$/C. *RSC Advances*, Volume 3(10), pp. 3421–3427

Chung, S.-Y., Bloking, J.T., Chiang, Y.-M., 2002. Electronically Conductive Phospho-Olivines as Lithium Storage Electrodes. *Nature Materials*, Volume 1, pp. 123–128

Deng, H., Jin, S., He, X., Zhan, L., Qiao, W., Ling, L., 2012. $LiFePO_4$/C Nanocomposites Synthesized from Fe_2O_3 by a Hydrothermal Reaction-calcination Process and Their Electrochemical Performance. *Journal of Inorganic Materials*, Volume 27(9), pp. 997–1002

Franger, S., Le Cras, F., Bourbon, C., Rouault, H., 2003. Comparison Between Different LiFePO4 Synthesis Routes and Their Influence on Its Physico-Chemical Properties. *Journal of Power Sources*, Volume 119-121, pp. 252–257

Han, X., Ouyang, M., Lu, L., Li, J., 2014. Cycle Life of Commercial Lithium-ion Batteries with Lithium Titanium Oxide Anodes in Electric Vehicles. *Energies*, Volume 7(8), pp. 4895–4909

Hsu, K.-F., Tsay, S.-Y., Hwang, B.-J., 2004. Synthesis and Characterization of Nano-sized $LiFePO_4$ Cathode Materials Prepared by a Citric Acid-Based Sol-gel Route. *Journal of Materials Chemistry*, Volume 14(17), pp. 2690–2695

Li, B., Ning, F., He, Y.-B., Du, H., Yang, Q.-H., Ma, J., Kang, F., Hsu, C.-T., 2011. Synthesis and Characterization of Long Life $Li_4Ti_5O_{12}$/C Composite using Amorphous TiO_2 Nanoparticles. *International Journal of Electrochemical Science*, Volume 6, pp. 3210–3223

Nagakane, T., Yamauchi, H., Yuki, K., Ohji, M., Sakamoto, A., Komatsu, T., Honma, T., Zou, M., Park, G., Sakai, T., 2012. Glass–ceramic $LiFePO_4$ for Lithium-ion Rechargeable Battery. *Solid State Ionics*, Volume 206, pp. 78–83

Padhi, A., Nanjundaswamy, K.S., Masquelier, C., Okada, S., Goodenough, J.B., 1997. Effect of Structure on the Redox Fe^{3+}/Fe^{2+} in Iron Phosphate. *Journal of the Electrochemical Society*, Volume 144(5), pp. 1609–1613

Shu, H., Wang, X., Wu, Q., Liang, Q., Yang, X., Yang, S., Liu, L., Wei, Q., Hu, B., Zhou, M., Chen, M., Zhang, L., 2012. Enhancement of Electrochemical Properties for Monodisperse Spherical $LiFePO_4$/C Synthesized by Ammonia Assisted Hydrothermal Route via Ni and F Co-doping. *Journal of the Electrochemical Society*, Volume 159(11), pp. A1904–A1911

Tan, Q., Lv, C., Xu, Y., Yang, J., 2014. Mesoporous Composite of $LiFePO_4$ and Carbon Microspheres as Positive-electrode Materials for Lithium-ion Batteries. *Particuology*, Volume 17, pp. 106–113

Teng, T.-H., Yang, M.-R., Wu, S.-h., Chiang, Y.-P., 2007. Electrochemical Properties of $LiFe_{0.9}Mg_{0.1}PO_4$/carbon Cathode Materials Prepared by Ultrasonic Spray Pyrolysis. *Solid State Communications*, Volume 142(7), pp. 389–392

Väyrynen, A., Salminen, J., 2012. Lithium Ion Battery Production. *J. Chem. Thermodynamics*, Volume 46, pp. 80–85

Wang, D., Wu, X., Zhang, Y., Wang, J., Yan, P., Zhang, C., He, D., 2014. The Influence of the TiO_2 Particle Size on the Properties of $Li_4Ti_5O_{12}$ Anode Material for Lithium-ion Battery. *Ceramics International*, Volume 40(2), pp. 3799–3804

Wang, Q., Deng, S., Wang, H., Xie, M., Liu, J.B., Yan, H., 2013. Hydrothermal Synthesis of Hierarchical $LiFePO_4$ Microspheres for Lithium Ion Battery. *Journal of Alloys and Compounds*, Volume 553, pp. 69–74

Yang, J., Xu, J.J., 2004. Nonaqueous Sol-gel Synthesis of High-performance $LiFePO_4$. *Electrochemical and Solid-State Letters*, Volume 7(12), p. A515–A518

Yang, M.R., Ke, W.H., 2008. The Doping Effect on the Electrochemical Properties of $LiFe_{0.95}M_{0.05}PO_4$ ($M = Mg^{2+}$, Ni^{2+}, Al^{3+}, or V^{3+}) as Cathode Materials for Lithium-ion Cells Batteries and Energy Storage. *J. Electrochem. Soc.*, Volume 155, pp. A729–A732

Yang, X., Hu, Z., Liang, J., 2015. Effects of Sodium and Vanadium Co-doping on the Structure and Electrochemical Performance of $LiFePO_4$/C Cathode Material for Lithium-ion Batteries. *Ceramics International*, Volume 41(2), pp. 2863–2868

Yu, W., Wu, L., Zhao, J., Zhang, Y., Li, G., 2014. Hydrothermal Synthesis of Spindle-shape and Craggy-faced $LiFePO_4$/C Composite Materials for High Power Li-ion Battery. *Advanced Powder Technology*, Volume 25(6), pp. 1688–1692

Zhong, M.-e., Zhou, Z., 2010. Effect of Reactant Phase form on the Properties of $LiFePO_4$ Synthesized by Carbothermal Reduction Method. *Solid State Ionics,* Volume 181(35-36), pp. 1607–1610

Zhou, N., Wang, H.-Y., Uchaker, E., Zhang, M., Liu, S.-Q., Liu, Y.-N., Cao, G., 2013. Additive-Free Solvothermal Synthesis and Li-ion Intercalation Properties of Dumbbell-shaped LiFePO4/C Mesocrystals. *Journal of Power Sources*, Volume 239, pp. 103–110